Proceedings of ICMM2005
3rd International Conference on Microchannels and Minichannels
June 13-15, 2005, Toronto, Ontario, Canada

ICMM2005-75159

CFD SIMULATIONS OF GAS AND LIQUID SLUGS FOR TAYLOR FLOW IN A MICROCHANNEL

Dongying Qian, Adeniyi Lawal
Department of Chemical, Biomedical and Materials Engineering
Stevens Institute of Technology, Castle Point on Hudson, Hoboken, NJ 07030, USA

ABSTRACT

The rapid development of microfabrication techniques creates new opportunities for applications of microchannel reactor technology in chemical reaction engineering. The extremely large volume-to-surface ratio and the short transport path in microchannels enhance heat and mass transfer dramatically and hence provide many potential opportunities in chemical process development and intensification. Multiphase reactions involving gas/liquid reactants with a solid as a catalyst are ubiquitous in the chemical and pharmaceutical industries, and the hydrodynamics play a prominent role in reactor design and performance. For gas/liquid two-phase flow in a microchannel, the Taylor slug flow regime is the most commonly encountered flow pattern, therefore the present study deals with the numerical simulation of gas and liquid slugs in a microchannel. A T-junction microchannel (empty or packed) with varying cross-sectional width (0.25, 0.5, 0.75, 1, 2 and 3 mm) served as the model micro-reactor, and a finite volume based commercial CFD package, FLUENT, was adopted for the numerical simulation. The gas and liquid slug lengths at various operating conditions were obtained and found to be in good agreement with the literature data.

Keywords: Taylor flow; Liquid and gas slugs; Microchannel; Numerical simulation

INTRODUCTION

The microchannel reactor has many advantages over conventional macroreactors. With its small transverse dimensions (submillimeter), the microchannel reactor possesses extremely high surface to volume ratios, and consequently exhibits enhanced heat and mass transfer rates. Scale-up for high throughput is achieved by simple replication of microreactor units; which eliminates costly reactor redesign and pilot plant experiments, thus shortening the development time from laboratory to commercial production. There are numerous potential applications for microchannel reaction technology in chemical and biological engineering, which are suitable for various types of reactions, from thin-wall reactors, membrane reactors to packed bed reactors, and from single phase reactions to multiphase reactions (Jensen 2001).

Multiphase flow finds applications in many industrially important chemical processes such as gas-liquid hydrogenation and immiscible liquid-liquid nitration. Since the flow in a microchannel is typically laminar, the mass transfer between the phases is mainly dominated by diffusion, and turbulent convective flow normally relied upon for rapid and effective mixing in macroreactors is non-existent. Mixing is therefore a critical issue in the design of multiphase microreactors. Over a wide range of operating conditions, the flow in a multiphase microchannel is typically the so-called Taylor flow regime (Heiszwolf et al. 2001). Taylor flow is a special case of slug flow where the bullet-shaped bubbles (Taylor bubbles) are separated by free-gas-entrained liquid slugs. The elongated bubble has a characteristic capsular shape with equivalent diameter larger than the channel width. There is a very thin film between the gas bubble and the channel wall. Taylor slug flow has been shown to increase transverse heat and mass transfer compared to single phase laminar flow because of the recirculation within the liquid slugs and the reduction of axial mixing between the liquid slugs (Bercic & Pintar 1997, Irandoust & Andersson 1989). A number of studies on mass transfer in Taylor flow in a microchannel have been carried out both experimentally and numerically (Bercic & Pintar 1997, Irandoust & Andersson 1988, Kreutzer et al. 2001, van Baten & Krishna 2004, van Baten & Krishna 2005). Several empirical correlations of mass transfer coefficients from gas phase to liquid phase, liquid phase to solid phase and gas phase to solid phase through the liquid film have been proposed (Bercic & Pintar 1997, Kreutzer et al. 2001). These mass transfer coefficients are mainly determined by the hydrodynamic characteristics of the flow with the gas and liquid slug lengths playing a very important role.

The slug length depends upon flow velocity, channel geometry and fluid properties. In microchannels, the buoyancy effect is suppressed by surface tension, which in effect renders the flow characteristic independent of channel orientation with respect to gravity (Triplett et al. 1999). The hydrodynamic characteristics of the flow in microchannels are different from those encountered in ordinarily large-size channels. The threshold of hydraulic channel diameter is about 1mm with fluid properties similar to air and water (Akbar et al. 2003). Although many investigators have characterized the flow

regimes in microchannels (Chen et al. 2002, Chung & Kawaji 2004, Triplett et al. 1999, Yang & Shieh 2001, Fukano & Kariyasaki 1993, Coleman & Garimella 1999, Akbar et al. 2003, Thulasidas et al. 1997), and some numerical studies on bubble velocity and profile have been performed (Tata & Cui 2004, Smith et al. 2002), however, based on our literature review, there are no numerical studies focusing on the hydrodynamics of gas and liquid slugs in microchannels.

The present work studies the development of gas and liquid slugs in a model T-junction microreactor at various operating conditions (measurable superficial parameters). A finite volume based commercial Computational Fluid Dynamics (CFD) package, FLUENT, was adopted for the numerical simulations. The major objective of the present work is to use CFD tool to study the hydrodynamics of the Taylor slug flow inside microchannels in order to provide some physical insights into the mass transfer mechanisms of the slug flow.

NOMENCLATURE

d	internal channel width, m
d_p	particle size in the packed bed, m
F	body force, N
L	mean slug length, m
$\tilde{L}$	in-situ slug length, m
N	number of slugs
N_0	total number of slugs
g	gravity, kg/m^2
p	system pressure, Pa
t	time, s
U	superficial velocity, m/s
v	velocity, m/s

Greek letters

α	volume fraction
β	porous medium permeability (m^2)
ε	void fraction of the packed bed
ε_L	liquid hold-up
κ	curvature (1/m)
μ	molecular viscosity, kg/m s
θ	contact angle, ^{o}
ρ	density, kg/m^3
σ	surface tension, N/m

Subscripts

G	gas
L	liquid
min	minimum
max	maximum
exp	experiment

1. Analysis

Model geometry

Figure 1 is the model T-junction microchannel reactor used in our flow simulation: a stream of water and a stream of air are fed separately into the two inlets of the mixing section, and then enter the reaction zone. The bed is either empty (wall surface reaction) or packed with solid particles (packed bed reactor). The cross-sectional dimension of the channel is d. The mixing section has a length of 6d while the reactor zone has a length of 60d. "Cold" flow without any chemical reactions is considered. The whole system is maintained at room temperature and the pressure is atmospheric at the exit. The superficial gas velocity as well as superficial liquid velocity varies from 0.01 to 0.25 m/s. According to the flow regime maps by Chung & Kawaji 2004, Triplett et al. 1999, Yang & Shieh 2001, Fukano & Kariyasaki 1993, Coleman & Garimella 1999 and Akbar et al. 2003, at these operating conditions, the flow falls within the Taylor slug regime. Four submillimeter channel diameters, namely 0.25, 0.50, 0.75, 1.0 mm, and two millimeter-size channel diameters, 2.0, 3.0mm, are chosen for the simulations.

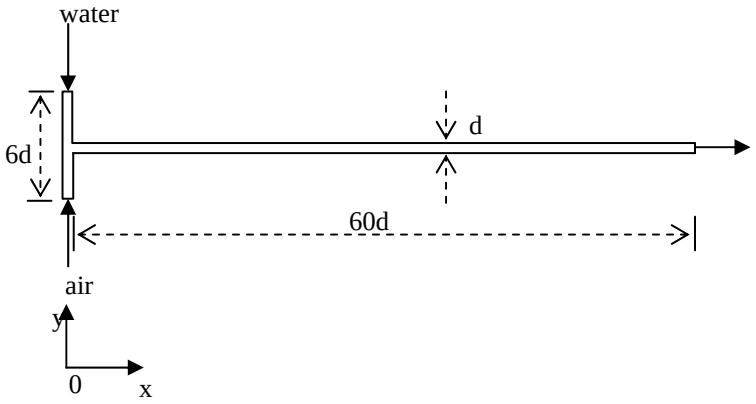

Fig. 1. Model T-junction microchannel used in the simulation

Governing equations

The CFD package FLUENT (Release 6.1.22, 2003) was used to perform the numerical simulations. FLUENT offers flow, heat and mass transfer modeling suited to a wide range of applications. In order to track the interface between the gas and liquid slugs, one of the general multiphase models in FLUENT, the volume of fluid (VOF) model, is adopted to simulate the Taylor slug flows in the T-junction microchannel. The governing equations of the VOF formulations on multiphase flows are as follows:

Equation of continuity:

$$\frac{\partial \rho}{\partial t} + \nabla \cdot (\rho \vec{v}) = 0 \quad (1)$$

Equation of motion:

$$\frac{\partial (\rho \vec{v})}{\partial t} + \nabla \cdot (\rho \vec{v} \vec{v}) = -\nabla p + \nabla \cdot [\mu (\nabla \vec{v} + \nabla \vec{v}^T)] + \rho \vec{g} + \vec{F} \quad (2)$$

Volume fraction equation:

$$\frac{\partial \alpha_G}{\partial t} + \vec{v} \cdot \nabla \alpha_G = 0 \quad (3)$$

where

$$\rho = \alpha_L \rho_L + \alpha_G \rho_G \, , \mu = \alpha_L \mu_L + \alpha_G \mu_G \quad (4)$$

Compared to single phase flow simulations, the VOF method accomplishes interface tracking by solving additional continuity-like equation(s) for the volume fraction (n-1 equations with n as the number of phases) (Hirt and Nicholas, 1981). For gas-liquid two phase flows, the volume fraction of gas α_G is obtained by numerically solving Eq. (3), and the volume fraction of liquid α_L is simply computed from 1-α_G. However, the implementation of the VOF model is numerically challenging. First, both the density ρ and viscosity μ in Eqs. (2), and (3) are mixture properties, which vary within the flow domain and are computed by the volume fraction weighted average. Second, the interface needs to be constructed based on the computed value of the volume fraction with the application of interpolation schemes for the identification of the interface. Third, surface tension along the interface between each pair of phases, and wall adhesion between the phases and the walls become very important for some cases, especially when the gravitational effect is negligible. All these complexities make VOF multiphase flow simulation computationally expensive, and convergence difficult to achieve when compared to its single phase counterpart.

Numerical approach

The flow inside the microchannel is essentially laminar. Typically, surface tension force dominates over the gravitational effect, and wall adhesion force is also important. In FLUENT, the surface tension model is the continuum surface force (CSF) model proposed by Brackbill et al (1992). With this model, the addition of surface tension to the VOF calculation results in a source term in the momentum Eq. (2) (FLUENT, 2003). In the case of wall adhesion, a contact angle needs to be specified. Rather than impose the boundary condition at the wall itself, the contact angle that the fluid is assumed to make with the wall is used to adjust the surface normal in cells near the wall. This so-called dynamic boundary condition results in the adjustment of the curvature of the surface near the wall, and this curvature is then used to adjust the body force term in the surface tension calculation (FLUENT, 2003). If the solid particles are present in the bed, the porous media model in FLUENT is used. The porous media model incorporates an empirically determined flow resistance in a region of the model defined as ``porous''. Essentially, the porous media model is nothing more than an added momentum sink in the governing momentum equations (FLUENT, 2003).

For gas-liquid two phase flow, the source term in Eq. (2) that arises from surface tension can be computed by the following:

$$\vec{F} = \sigma \frac{2\rho\kappa_G \nabla \alpha_G}{(\rho_G + \rho_L)} \quad (5)$$

where κ is the curvature computed from the divergence of the unit surface normal. The source term due to the porous medium is calculated from:

$$\vec{F} = -\frac{\mu \vec{v}}{\beta} = -\frac{150\mu(1-\varepsilon)}{d_p^2 \varepsilon^3} \vec{v} \quad (6)$$

where 1/β is viscous resistance, β is the permeability of the porous medium, d_p is the particle size in the packed bed, and ε is the void fraction of the bed.

The model geometry was meshed with the preprocessor GAMBIT software (part of FLUENT package), then imported into processor FLUENT for calculation. The simulation results were either analyzed by FLUENT integrated postprocessor or exported into data files for other postprocessor packages. For the model geometry Fig. 1, a 3D circular tube, a 3D rectangular duct and a 2D rectangular duct were simulated at the same operating conditions. The results indicated no significant difference in the gas and liquid slug lengths for the three configurations. Therefore, the data shown hereafter were all for 2D simulation results. A uniform rectangular grid was used in the simulations. A series of mesh cells with different fineness were chosen until the results did not show significant changes. There were 3087 rectangular cells in the model geometry for the data presented in this work.

A segregated time dependent unsteady solver was used. The boundary conditions are: velocity inlet for the inlets, and outflow for the outlet. The other options selected in FLUENT were as follows: the PRESTO! (PREssure STaggering Option) scheme for the pressure interpolation**,** the PISO (Pressure-Implicit with Splitting of Operators) scheme for the pressure-velocity coupling, second-order up-wind differencing scheme for the momentum equation, the geometric reconstruction scheme for the interface interpolation, implicit body force treatment for the body force formulation, and Courant number 0.25 for the volume fraction calculation. In addition, the time step, the maximum number of iterations per time step, and the relaxation factors needed to be carefully adjusted to ensure convergence.

A total of about 500 simulation runs with varying parameter values: channel diameter d, superficial gas velocity U_G, superficial liquid velocity U_L, surface tension σ, liquid viscosity μ_L, porous medium permeability β and wall contact angle of liquid θ, were carried out on Linux PC cluster with 2.8GHz Pentium IV or Xeon processors. A few thousand to ten thousand time steps were required for each run. A typical run took about 24 hours. Twenty to a hundred slugs were collected, from which the sample averages and other statistical information were computed. Unless otherwise stated, the data presented in the following sections are for an empty bed with surface tension of 0.072 N/m, a liquid viscosity of 0.001 kg/ms and wall contact angle of liquid of 0^o.

2. Results and Discussion

Comparison of experimental data with numerical predictions

As earlier stated, most of the literature studies characterized the flow patterns and presented the flow regime maps inside the microchannels. Though there were a few pictures of the slug flows in these studies (Chen et al. 2002, Chung & Kawaji 2004, Triplett et al. 1999, Yang & Shieh 2001, Fukano & Kariyasaki 1993, Coleman & Garimella 1999), no corresponding slug length data were presented. Laborie et al. (1999) presented some experimental data about the gas and liquid slug lengths inside capillaries. However, the air was introduced into the water through a porous membrane, rather than through a Tee mixer. According to our simulation, the premixed degree of the gas and the liquid strongly affects the slug length, while the length of the mixer or the reactor has no effect on the slug length as long as it is long enough to obtain a fully developed flow. Vandu et al. (2004) conducted air-water flow visualization experiments in a 1.4 m long vertical Pyrex glass capillary through a 3 mm T-Junction mixer. Five different capillaries, circular capillaries with internal diameters of 0.91, 2 and 3.02 mm and square capillaries with internal hydraulic diameters of 0.99 and 2.89 mm, were used in their experiments. The video zoom is in the midway and the measuring focus distance is about 0.2 m. From the sample movies posted on their website for 3.02 mm capillary tube, we were able to obtain the slug length information. Table 1 lists our simulation results and their experimental data. It can be seen that the simulations are consistent with the experiments.

Table 1
Comparison between numerical simulations and experiments in a 3 mm vertical circular capillary

U_G (m/s)	U_L (m/s)	L_G (mm)	L_{Gmin} (mm)	L_{Gmax} (mm)	L_L (mm)	L_{Lmin} (mm)	L_{Lmax} (mm)
			L_{Gmin} (exp.)	L_{Gmax} (exp.)		L_{Lmin} (exp.)	L_{Lmax} (exp.)
0.05	0.02	15.38	13.95	16.65	7.28	6.30	8.10
			13.00	*15.00*		*4.95*	*9.45*
0.05	0.05	12.80	12.15	13.50	12.47	11.25	13.50
			12.00	*13.00*		*12.00*	*13.00*
0.05	0.10	6.22	3.60	9.45	9.39	3.15	18.90
			3.50	*9.50*		*6.00*	*18.50*
0.05	0.15	4.56	2.25	9.45	9.10	2.25	20.25
			3.00	*8.50*		*3.00*	*25.00*
0.05	0.20	3.30	1.35	8.10	7.48	1.35	22.05
			2.00	*9.50*		*1.50*	*38.00*
0.10	0.02	19.19	6.75	32.85	3.98	1.80	7.65
			20.50	*31.00*		*3.00*	*5.00*
0.10	0.05	15.39	9.45	18.90	5.64	2.25	8.55
			17.00	*18.50*		*6.50*	*7.50*
0.10	0.10	5.55	4.50	13.50	3.22	1.35	8.10
			10.00	*13.50*		*7.50*	*11.00*
0.10	0.15	4.98	3.60	10.35	4.50	2.25	9..90
			3.50	*13.00*		*2.00*	*15.50*
0.10	0.20	4.93	2.25	8.55	6.42	1.35	12.60
			3.00	*9.00*		*1.50*	*24.00*

In Table 1, L_G and L_L are sample average values (time and space mean values). Both simulation results and experimental data indicate that the slug length is not uniform throughout the channel length because of the time-dependent toroidal vortices generated when the two streams meet at the mixing section and which subsequently propagate throughout the length of the channel. This non-uniformity becomes more pronounced as the superficial gas or liquid velocity increases. Figure 2 shows five snapshot flow patterns at different liquid flow rates. These simulations confirm that for all the above operating conditions, the flow in each case is in the Taylor slug regime. The non-uniformity of the slugs can be clearly seen in Fig. 2. Figure 3 is the bar plot of in-situ gas and liquid slug length distributions corresponding to these cases, where N is the number of slugs at a paticular size range, and N_0 is the total number of slugs. As one observes, the slug length variation becomes wider as the liquid flow rate increases.

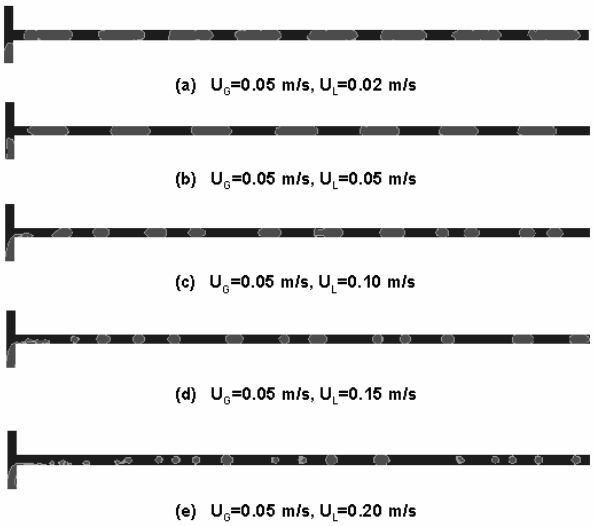

Fig. 2. Contour plots of volume fraction of air in a 3 mm vertical circular capillary
(grey —— gas slug, black —— liquid slug)
(gravity direction: -x)

Influence of gas and liquid superficial velocities

The influence of gas and liquid superficial velocities on the gas and liquid slug lengths was studied. Figure 4 shows the relationship between the gas slug length and the superficial velocities, while Figure 5 shows corresponding behavior for the liquid slug length. The gas slug grows with increase in superficial gas velocity and decrease in superficial liquid velocity. Similar trend is observed for the liquid slug length, i,e, it increases with increase in superficial liquid velocity, and decrease in superficial gas velocity. This trend is consistent with experimental observations of Larborie et al. (1999) who reported a linear relationship between L_G and U_G. Here, we use a power-law fit for all the sample data. In Figs. 4 and 5, the solid curves represent the fitted lines. For cross-sectional dimensions of 1mm and lower, the data are well described by one curve. For the computational geometries considered in this study, the 1 mm and submillimeter channels exhibit more uniform slugs than millimeter-size channels. The simulation data show more scatter for the 2mm and 3mm

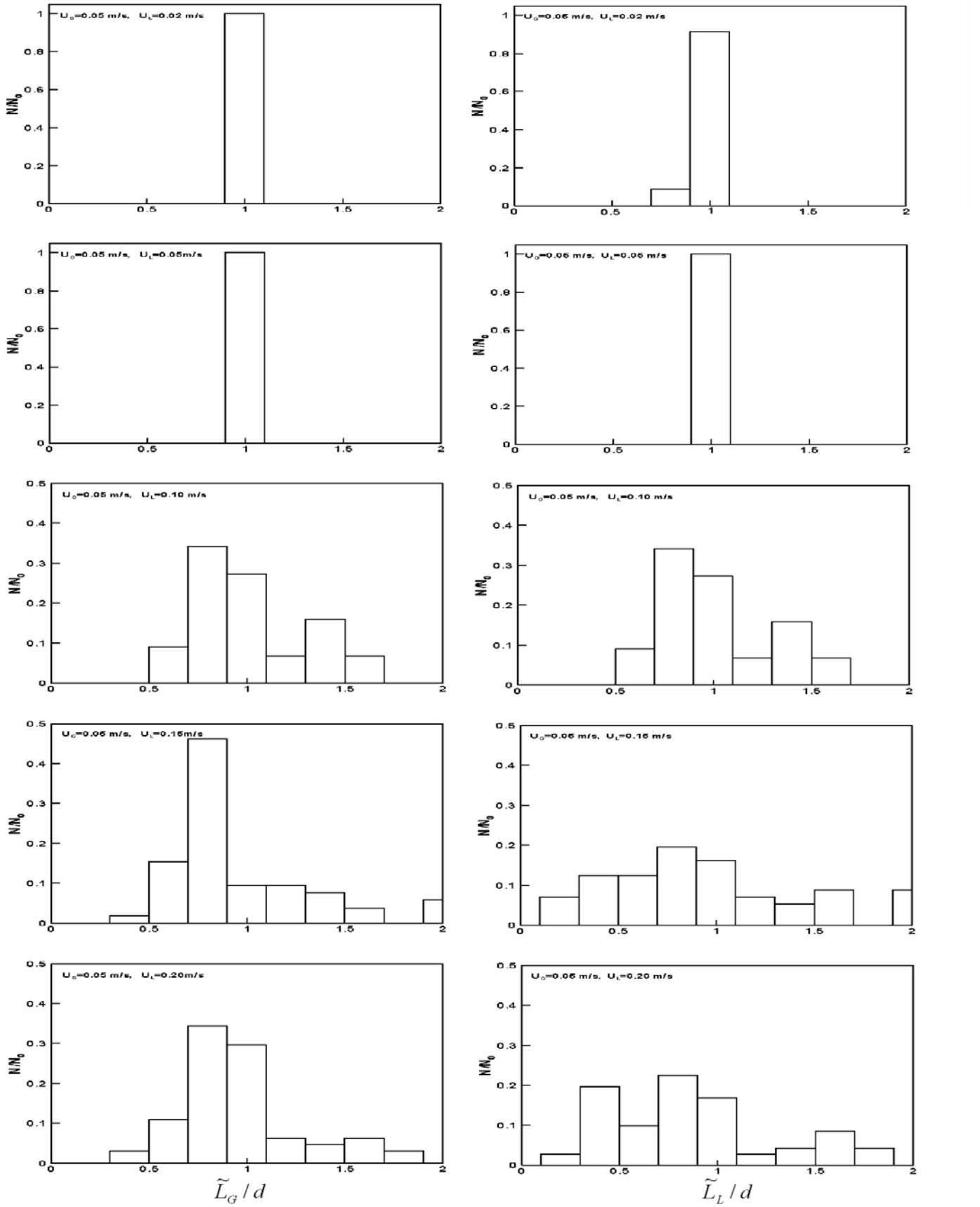

Fig. 3. Slug length distributions in a 3 mm vertical capillary tube

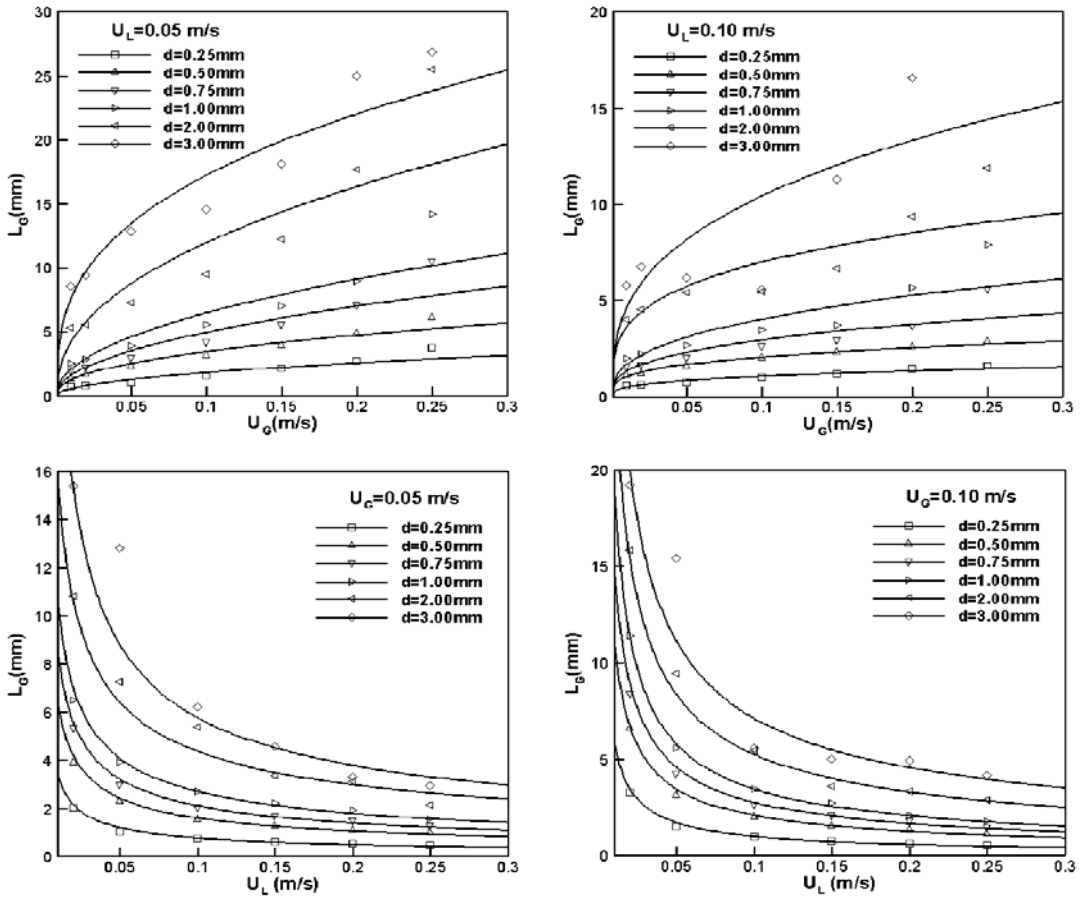

Fig. 4. Influence of gas and liquid superficial velocities on gas slug length

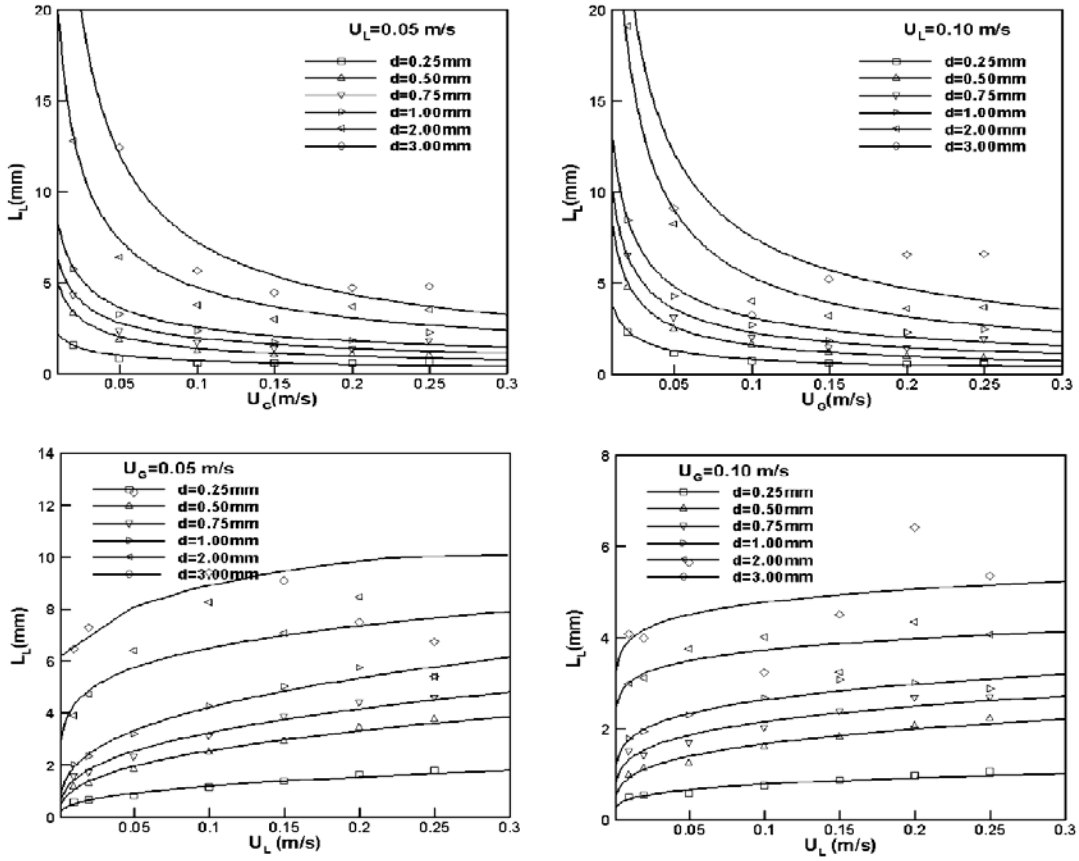

Fig. 5. Influence of gas and liquid superficial velocity on liquid slug length

channels. The effect of superficial liquid velocity on gas slug length, and the effect of superficial gas velocity on liquid slug length are more remarkable. The higher the gas proportion, the longer the gas slugs. Similar observation applies to the liquid slugs.

Figures 4 and 5 also show the influence of the channel width on the gas and liquid slug lengths: at the same superficial gas and liquid velocities, a wider channel has longer gas and liquid slugs. Figure 6 depicts the relationship between the dimensionless liquid slug length L_L/d and the liquid hold-up ε_L while Figure 7 shows the dimensionless unit cell length $(L_G+L_L)/d$ as a function of the liquid hold-up ε_L. Here we simply assume the liquid flow rate volume fraction $U_L/(U_G+U_L)$ as approximately equal to the liquid hold-up ε_L. As we can see, the simulation data collapse well on smooth curves. To make further comparisons, we have also plotted the experimental results of Heiszwolf et al. (2001) from 0.5 ~ 5 mm monolith reactors with air and water. Our simulation results are in good agreement with their experimental data. When the liquid hold-up is within a certain range ($0.25< \varepsilon_L <0.75$), both the dimensionless slug length and unit cell length can be considered constant (2 and 4 respectively).

Influence of packing conditions in a packed bed

We also investigated slug flow in a packed bed. Figure 8 shows the gas and liquid slug lengths in 0.25, 0.50, and 0.75 mm packed bed with 50 micron particles at different void fraction values. Here the gas and liquid velocities are based on real void volume (physical velocity). We can see that as the particles become more densely packed, the slug length decreases.

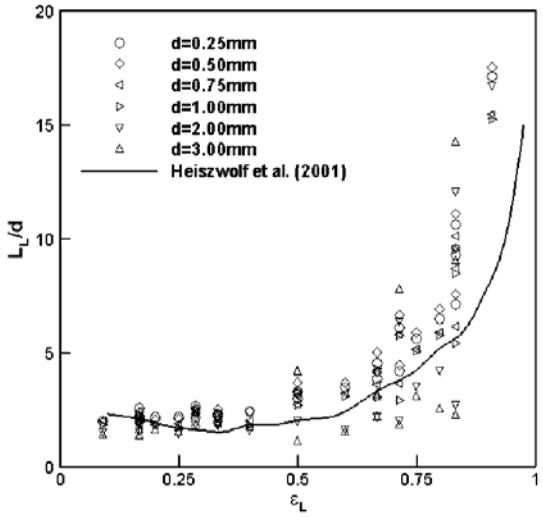

Fig. 6. Dimensionless liquid slug length vs. liquid hold-up

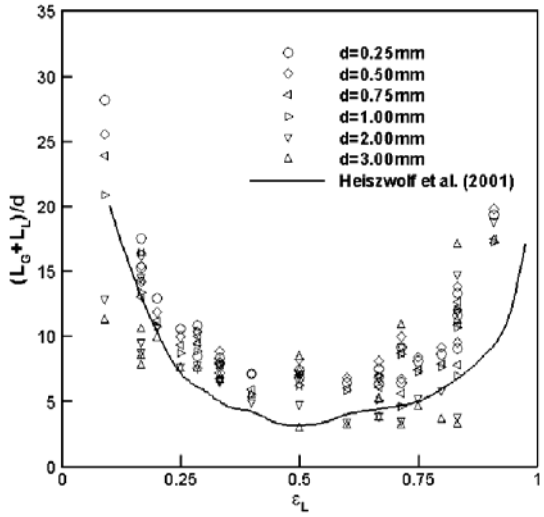

Fig. 7. Dimensionless unit cell length vs. liquid hold-up

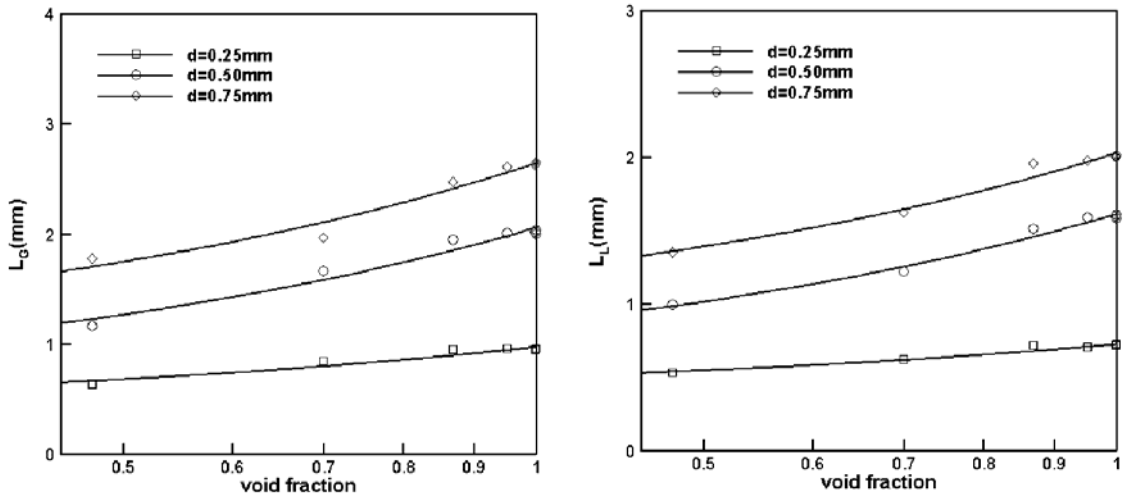

Fig. 8. Slug length in a bed packed with 50 micron particles at different void fraction (U_G=0.1 m/s, U_L=0.1 m/s)

3 Conclusions

The characteristics of Taylor slug flow in microchannels have been elucidated using CFD simulation. The gas and liquid slug lengths were calculated for various operating conditions. The slug length is not uniform throughout the channel especially for channel cross-sectional dimensions exceeding 1 mm. When the gas or liquid flow rate increases, the slug non-uniformity becomes more pronounced. The gas slug length increases with increase of superficial gas velocity, and decrease of superficial liquid velocity. The liquid slug length increases with increase of superficial liquid velocity, and decrease of superficial gas velocity. Wider channels have longer slug length at the same superficial gas and liquid velocities. In a certain liquid hold-up range, the dimensionless slug length is about 2.

Based on this study of Taylor flow, we can begin to understand and quantify heat and mass transfer enhancement in microchannels, which will be the subject of our next study.

ACKNOWLEDGMENTS

The authors gratefully acknowledge the financial support from Department of Energy-OIT under grant Nos. DE-FC36-021D14427 and DE-FC36-03G013156

REFERENCES

Akbar, M.K., Plummer, D. A., Ghiaasiaan, S.M., 2003. On gas-liquid two-phase flow regimes in microchannels. International Journal of Multiphase Flow. 29, 855-865.

Bercic, G., Pintar, A., 1997. The role of gas bubbles and liquid slug lengths on mass transport in the Taylor flow through capillaries, Chemical Engineering Science 52(21/22), 3709-3719.

Brackbill, J.U., Kothe, D.B., Zemach, C.,1992. A continuum method for modeling surface tension, Journal of Computational Physics 100, 335-354.

Chen, W.L., Twu, M.C., Pan, C., 2002. Gas-liquid two-phase flow in micro-channels. International Journal of Multiphase Flow 28, 1235-1247.

Chung, P.M.-Y., Kawaji, M. 2004. The effect of channel diameter on adiabatic two-phases flow characteristics in microchannels. International Journal of Multiphase Flow 30, 735-761.

Coleman, J. W., Garimella S., 1999. Characterization of two-phase flow patterns in small diameter round and rectangular tubes. International Journal of Heat and Mass Transfer 42, 2869-2881.

FLUENT 6.1 documentation, 2003. Fluent Incorporated, Lebanon, New Hampshire.

Heiszwolf, J.J., Kreutzer, M.T., van den Eijnden, M.G., Kapteijn, F., Moulijn, J.A., 2001. Gas-liquid mass transfer of aqueous Taylor flow in monoliths. Catalysis Today 69, 51-55.

Fukano, T., Kariyasaki, A., 1993. Characteristics of gas-liquid two-phase flow in a capillary tube. Nuclear Engineering and Design 141, 59-68.

Hirt, C.W. , Nicholas, B.D., 1981. Volume of fluid (VOF) method for the dynamics of free boundaries. Journal of Computational Physics 39, 201-225.

Irandoust, S. , Andersson, B., 1988. Mass transfer and liquid-phase reactions in a segmented two-phase flow monolithic catalyst reactor. Chemical Engineering Science 43(8), 1983-1988.

Irandoust, S. , Andersson, B., 1989. Simulation of flow and mass-transfer in Taylor flow through a capillary. Computers Chemical Engineering 13(4/5), 519-526.

Jensen, K.F., 2001. Microreaction engineering — is small better? Chemical Engineering Science 56, 293-303.

Kreutzer, M.T., Du, P., Heiszwolf, J.J., Kapteijn F., Moulijn J. A., 2001. Mass transfer characteristics of three-phase monolith reactors. Chemical Engineering Science 56, 6015-6023.

Laborie, S. , Cabassud, C. , Durand-Bourlier, L., Laine, J. M. , 1999. Characterization of gas-liquid two-phase flow inside capillaries. Chemical Engineering Science 54, 5723-5735.

Smith, S., Taha, T., Cui, Z.F., 2002. Enhancing hollow fibre ultrafiltration using slug-flow — a hydrodynamic study. Desalination 146. 69-74.

Tata, T., Cui, Z.F., 2004. Hydrodynamics of slug flow inside capillaries. Chemical Engineering Science 59, 1181-1190.

Thulasidas, T.C., Abraham, M.A., Cerro, R.L., 1997. Flow patterns in liquid slugs during bubble-train flow inside capillaries. Chemical Engineering Science 52(17), 2947-2962.

Triplett, K.A., Ghiaasiaan, S.M., Abdel-Khalik, S.I., Sadowski, D.L., 1999. Gas-liquid two-phase flow in microchannels Part I: two-phase flow patterns. 25, 377-394.

Van Baten, J.M., Krishna, R., 2004. CFD simulation of mass transfer from Taylor bubbles rising in circular capillaries. Chemical Engineering Science 59, 2535-2545.

Van Baten, J.M., Krishna, R., 2005. CFD simulation of wall mass transfer for Taylor flow in circular capillaries. Chemical Engineering Science 59, 2535-2545.

Vandu, C. O., Liu, H., Krishna, R. , 2004. Taylor bubble rise in circular and square capillaries. University of Amsterdam, Amsterdam, The Netherlands, the 20th of July 2004.http://ct-cr4.chem.uva.nl/singlecapillary/

Yang, C.-Y., Shieh, C.-C., 2001, Flow pattern of air-water and two-phase R-134a in small circular tubes. International Journal of Multiphase Flow 27, 1163-1177.